Adapted from *Geophys. J. Int. (1996)*, **124**, *756-776*

THERMAL AND HYDRAULIC ASPECTS OF THE KTB DRILL SITE

T. Kohl and L. Rybach
Institut für Geophysik, ETH-Hönggerberg, CH-8093 Zürich, Switzerland

SUMMARY

The extensive data sets obtained by the KTB (lithological and structural information, BHT values, temperature logs, rock thermal properties) provide a unique opportunity to construct realistic thermal models and thus to shed light on thermal conditions in the upper crust. Our numerical simulation study, a Swiss contribution to the German KTB drilling project, aims at the understanding of the steady-state thermal and hydraulic field in the surroundings of the KTB. The simulations consider state-of-the-art petrophysical aspects relevant for deep, pressurised and high temperature structures and were performed on discretised 2-D/3-D Finite Element meshes that contain topography, geologic structures and hydrogeologic features.

Our analysis of the KTB temperature field suggests three zones of particular geothermal setting: a low heat flow zone in the uppermost layers with a transition to high heat flow at 500 m depth, the underlying region accessed by the borehole with its characteristical uniform gradient, and the mid/lower crust that must be responsible for the high heat flow regime at the KTB site. The two first zones are treated in the present paper. A three-dimensional thermo-hydraulic model was set up in order to evaluate the first 2000 m including the uppermost 500 m low heat flow zone. This model incorporates the complex geologic information from the KTB pilot hole and topography-driven fluid flow. The lateral boundaries of the model were carefully chosen by analysing the flow pattern within a large, regional three-dimensional domain. The drilled section is analysed by a 2-D model using the available structural information. Due to dominating refraction effects, a careful temperature gradient analysis has to be carried out for such steeply dipping structures. Both models indicate a thermal regime dominated by diffusive heat transfer. Hydraulic flow seems to be important only for the uppermost (~400 m) part of the drilled depth section; our simulations do not support significant fluid circulation at greater depths. In the drilled section the rather uniform gradient and the pronounced vertical heat flow variations can now be explained.

Finally, the potential and the limitation of the analysis of heat flows and temperature gradients are demonstrated; Heat flow interpretations are conclusive only for nearly horizontally layered, isotropic geologic units. In steeply dipping and anisotropic formations the heat flow field is perturbed over a large distance (>1 km) around the point of interest. In such geologic units only the temperature gradient interpretation can provide reliable information on the surrounding material.

Keywords: heat flow, numerical modelling, thermal and hydraulic field, upper crust

1 INTRODUCTION

The main stage of the German Continental Deep Drilling (KTB) project started in 1987 with the objectives of determining the physical conditions and of revealing the geologic structures in deep crystalline rock. First, a 4000 m deep pilot hole (VB) was drilled, accompanied by large-scale data acquisition. Thereafter, the main hole (HB) was sunk, reaching its final depth of 9101 m in September 1994. As a Swiss contribution to the German KTB drilling project, the numerical simulation study described here aims at the understanding of the geothermal field in the surroundings of the KTB site. The work has been performed in co-operation with different KTB investigators.

The various datasets collected and analysed in the KTB field laboratory for the VB and the HB as well as investigations in the surroundings show the complex structure of this area. The main tectonic unit at the KTB location is the Hercynian Zone of

Erbendorf - Vohenstrauss (ZEV). The centre of this zone is characterised by steep, SW-dipping, alternating gneissic and metabasitic rock units. To the west, Mesozoic sedimentary cover rocks and to the NE, large granitic intrusions are found. Seismic sections and borehole data show eastward dipping cataclastic joint zones that can be correlated with surface topography. A detailed geologic description of the KTB site is given by Emmermann (1989).

The intention of the present study is to condense and integrate the available information into a numerical model that is based on state-of-the-art petrophysical aspects relevant to deep, pressurised, high temperature structures. The geothermal observables such as temperature, temperature gradient, thermal conductivity, heat production and the derived quantity heat flow represent the basis of our interpretational steady state approach. In addition to the thermal parameters assumptions on permeability distribution in crystalline rock were required. Correct choice of parameters should yield calculated temperature profile, vertical temperature gradient and heat flow density in agreement with the observed values. In particular, the dependence of the data on strongly dipping alternating gneissic and metabasitic geologic units has been addressed.

In the following section a summary of those factors will be given that are likely to be relevant to the hydro-thermal situation at the KTB site.

2 GEOTHERMAL AND HYDRAULIC SITUATION

The thermal parameters measured in the KTB field laboratory provide an enormous data base on thermal conductivity and heat production. The petrophysical investigations differed in the VB and the HB operations: measurements could be performed during the VB phase on core samples, whereas only data from cuttings are available from the HB phase.

Besides the excellent thermal laboratory measurements on rock samples, only very poor temperature data are available from borehole measurements. The last complete temperature log in the VB was measured about 250 days after the drilling stopped. Because considerable activity took place in the borehole during these 250 days, deviations of this log from the conditions of the undisturbed thermal field must be expected. A second VB temperature log was conducted one year later but only down to a depth of 2000 m, where at that time a packer plugged the borehole. During the drilling phase of the HB, the most reliable temperature measurements indicating the undisturbed temperatures were obtained from BHT measurements made at about 1000 m intervals.

The heat flow values calculated from gradient and vertical thermal conductivity data (Huenges & Zoth, 1991) show an ambivalent feature: low values around 0.05 W m^{-2} in the upper 500 m, but at greater depths the values rise to 0.08 - 0.09 W m^{-2}. Below 1200 m, a nearly uniform thermal gradient of 0.028 K m^{-1} was derived from BHT measurements and temperature logs for the entire drilling depth. Therefore, high temperatures have been encountered at greater depth: a BHT measurement in 8110 m indicates 229°C. Obviously, the temperature field at the KTB is strongly influenced by the geologic structure, since the heat will preferentially flow along the near-vertical, better conducting gneissic formations with strongly anisotropic thermal conductivity (perpendicular to the foliation 3.0 W $m^{-1}K^{-1}$ and parallel to the foliation 3.6 W $m^{-1}K^{-1}$, see Huenges & Zoth 1991) rather than within the low-conductivity, isotropic metabasites (2.5 W $m^{-1}K^{-1}$).

The objective of heat flow modelling in the surroundings of KTB is to combine the laboratory datasets with standard geothermal simulations described for example in Chapman & Furlong (1992). The observation of different heat flow regimes at depth suggests that both the diffusive and the advective component of heat transport has to be addressed and evaluated. At least the following three zones in the KTB terrain are of particular geothermal interest:

- The upper 2000 m to investigate the uppermost low heat flow zone within a high heat flow regime.
- The drilled part of the upper crust down to 9000 m to explain the appearance of a uniform temperature gradient along with a strongly varying heat flow.
- The mid / lower crustal domain to explain the origin of the generally high heat flow regime.

The appearance of a low heat flow zone at the upper 500 m within a generally high heat flow regime was extensively studied and discussed in the literature. The low heat flow zone is in agreement with heat flow determinations that were performed in shallow boreholes for site investigation studies in the surroundings of the KTB. These boreholes indicated low values in the range of 0.04 to 0.075 W m^{-2}, and led to erroneously low temperature predictions at depth (Burkhardt et al, 1991). The considerations of Jobmann & Clauser (1994) and Rybach (1992) are important for the characterisation of this feature. According to these authors, the low heat flow zone at shallow depth could either be due to paleoclimatic effects, to the influence of hydraulically driven advection or to a combination of both.

A detailed study of the appearance of a low heat flow zone in a regional high heat flow regime is important since it can possibly prevent future misinterpretations of heat flow data from shallow boreholes. The present study focuses on this problem by a regional, combined thermo-hydraulic 3-D model of the uppermost 2000 m that incorporates topography effects as possible driving mechanisms for advective transport. Topography represents the strongest factor influencing the near surface hydraulic pressure field. A topographic map of the vicinity of the KTB (altitude 505 m) within a 10 km radius is shown in Fig. 1. It can be seen that the altitudes range from 950 m in the Fichtelgebirge to 400 m in the lower plains of the sedimentary cover rocks. The significance of hydraulic impact on the thermal field was highlighted recently by Jobmann & Clauser (1994) who performed two-dimensional calculations along a NE-SW profile running through the KTB site. They also identified a hydraulically influenced temperature field at various other, shallower boreholes located in the surroundings of the KTB. Based on one-dimensional Peclet number analysis they conclude that the boreholes located in crystalline rock (i.e. north-east of the Frankonian Line) are characterised by downward percolating fluids whereas the only available borehole west of the Frankonian Line is characterised by rising fluids. After correcting for the hydraulic effect all boreholes yield a higher basal heat flow than the raw data.

In the present paper, this uppermost zone is evaluated by means of a detailed 3-D model. It is intended to elucidate thermal and hydraulic effects by means of a detailed geologic and topographic description.

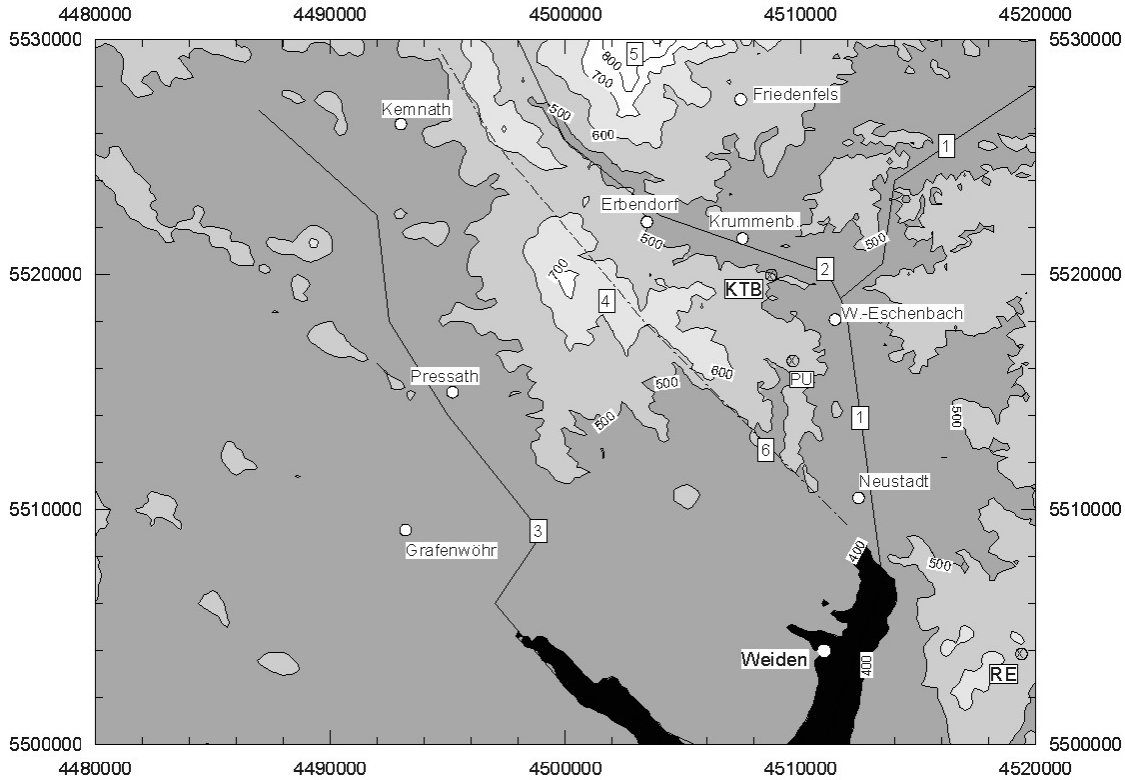

Figure 1. Topographic situation around KTB (isolines in m.a.s.l.). The coordinates correspond to the German coordinate system (in m). The topography is characterised by lower plains in the south and south-west and by increasing heights in the north of the KTB. The main features are indicated on the map by numbers: 1 - the Waldnaab river, 2 - the Fichtelnaab river in the valley near the KTB location which joins the Waldnaab, 3 - the Haidennaab river with sedimentary bedrock, 4 - the Kühberg, 5 - the heights of the southern Fichtelgebirge and 6 - the Frankonian Lineament (dashed line) that separates the crystalline block in the east from the SW situated sediments. All rivers discharge into the Danube, about 100 km south of Weiden. Also labelled on the map are the drillholes Püllersreuth (PU) and Remmersberg (RE) which were sunk during the site investigation study (see Burkhardt et al. 1989).

At greater depth, the hydraulic pressure field seems to be decoupled from near surface domains (Kessels et al., 1992) and influenced by fluid density variations due to higher salinity. Huenges (1993) showed that pressure measurements can be interpreted by an increase of density with depth, up to 1200 kg m^{-3} at 3000 m. The significance of pressure variation due to a permeability variation remains uncertain since borehole permeability measurements in the KTB do not indicate any significant variation with depth. The difference between laboratory scale and large scale measurements from the same depth extends over several orders of magnitude. Laboratory measurements on samples from intact rock show permeabilities around $10^{-20}m^2$, a hydraulic communication test over the 200 m distance between VB and HB revealed values on the order of $10^{-16}m^2$ (Kessels et al., 1992).

The second zone to be simulated represents the thermal field of the upper crust (< 10 km) that accounts for the complexity of the local geologic structures. Especially, the thermal effect of the steeply dipping geologic units was to be investigated. The drill core data from the VB reveal also the dipping angle of the geologic units as illustrated in Fig. 2. In the upper 2000 m with the steepest foliation, dips up to 90° can be found. Below a zone with rather shallow dip angle at around 3000 m the foliation dip increases again to about 60°. Simple, steady-state diffusive heat transport for the main part of the drilled section is assumed in this paper in the investigation of this feature. Our approach is to consider further heat transport mechanisms only if a successful

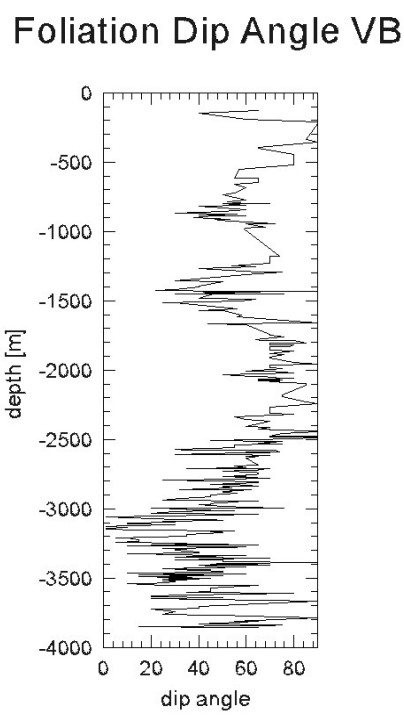

Figure 2. Dip of the geological units in the 4000 m deep VB drillhole.

diffusive simulation cannot be performed. The geologic model of the upper crust by Hirschmann (1993) is the basis of our study.

The simulation of thermal transport at greater depth (mid / lower crustal domain) and thereby the origin of the high heat flow must necessarily be more speculative. The Eger Graben (25 km NE of the KTB) represents a young tectonic perturbation and therewith a possible regional heat source. It is considered to be the juncture between the Hercynian Saxothuringian and Bohemian massifs. A deep reaching fault zone is indicated by the gas content of fluids. Fluids sampled from mineral springs at a fault zone near the SW border of the Eger Graben have a large portion of mantle derived helium (Weinlich et al., 1993). A further indication of mobile crustal fluids causing stress perturbations are seismic swarms with focal depths around 10 km (Dahlheim, 1993). The epicentres of these events are located about 20 km from the KTB near some basaltic occurrences, close to the SW border of the Eger Graben.

Subrecent volcanism is also known to originate from the Eger Graben. According to Kopecký (1986) three eruptions close to the Czech-German border represent the youngest volcanic event that dates 860000 years BP. Radiometric measurements indicate an even more recent age of approx.260000 years BP (Šibrava & Havlicek, 1980). The nearest event to the KTB is located at about 28 km to the E-NE. These volcanic events represent the latest manifestations of several episodes that started in early Miocene with the strongest activity some 25-20 Ma ago. The centre of that main episode was near Roztoky in the central Eger Graben. During early Miocene, the activity extended westward up to the sediments SW of the Frankonian Line. The likelihood of a thermal influence on the heat flow below the KTB will be evaluated in a separate study. The Eger Graben has already been mentioned by Burkhardt et al. (1991) in an analysis of possible regional heat sources. The authors are currently investigating this point (see some preliminary results in Kohl & Rybach, 1994), so that no further discussion will be given here.

Before a quantitative interpretation of the thermal regime in the two uppermost zones is presented, the thermal and hydraulic mechanisms considered as well as the discretisation procedure will be described.

3 TRANSPORT MECHANISMS IN DEEP CRYSTALLINE ROCK

The general porous medium approach was applied to treat mass and thermal transport in the realm under consideration. Diffusive thermal transport can be described with the Fourier equation,

$$\mathbf{q} = -\lambda \cdot \nabla T \qquad (1)$$

with **q** the heat flow vector, λ thermal conductivity, ∇ the Nabla operator, *T* the temperature.

Although λ generally is treated as a scalar, anisotropic effects can be approximated applying only the vertical component of thermal conductivity. At the KTB site with its steep dipping angles (60°-80°), off-diagonal terms of the real second rank thermal conductivity tensor are small compared to the vertical component ($\lambda_{zx}<\lambda_{zz}$ and $\lambda_{zy}<\lambda_{zz}$). Furthermore, lateral temperature gradients are negligible ($\partial T/\partial z >> \partial T/\partial x$, $\partial T/\partial z >> \partial T/\partial y$). Thus, the vertical component of the heat flow q_z that is the only measurable in vertical boreholes can be approximated by:

$$q_z = -\lambda_{zx} \cdot \partial T/\partial x - \lambda_{zy} \cdot \partial T/\partial y - \lambda_{zz} \cdot \partial T/\partial z \approx -\lambda_{zz} \cdot \partial T/\partial z \qquad (2)$$

For modelling purposes, the value of λ in a porous medium can be best approximated from cuttings or cores by applying the geometrical mean between the solid and the fluid phase (Pribnow, 1994). If not only diffusive but also advective thermal transport is considered the thermal energy equation for steady state can be written as:

$$\nabla \cdot (\lambda \cdot \nabla T) - \left[\rho c_p\right]_f \cdot \mathbf{v}_d \cdot \nabla T + H = 0 \qquad (3)$$

with $[rc_p]_f$ specific heat capacity of fluid, $\mathbf{v}_d$ the Darcy velocity and *H* the heat production rate.

The hydraulic pressure field is commonly described by combining mass conservation with Darcy's flow law. Its extended form can be given as follows:

$$\nabla \cdot \left(\frac{\rho_f \cdot g \cdot k}{\mu} \cdot \left[\nabla h - \frac{(\rho_f - \rho_{f0}) \cdot \nabla z}{\rho_{f0}} \right] \right) = 0 \qquad (4)$$

with m the dynamic fluid viscosity, *k* the matrix permeability, r_{f0} the reference fluid density, r_f the fluid density, g the gravity, ∇ *z* the vertical component of the unity vector and *h* the hydraulic head. The term $(r_f - r_{f0})\nabla z/r_{f0}$ describes the effect due to the density difference between reference density and in-situ density.

The physical conditions in deep crystalline rock are different from those near the surface or in the laboratory. This implies that in the above equations the temperature and pressure dependence of fluid and rock properties must be considered. The implications are manifold for a geothermal model in deeper regions of the crust, since several non-linear constitutive relationships have to be taken into account.

The non-linear dependence of the fluid parameters was derived from Phillips et al. (1981) who analysed the behaviour from brines for different databases. The dependence of rock thermal conductivity on temperature and pressure have been measured for example by Buntebarth (1991) and compiled by Clauser &

Huenges (1995). A preferred fitting curve for the decrease of conductivity with temperature is a hyperbolic function:

$$\lambda(T) = 1/(A + B \cdot T) \quad (4)$$

with *A*, *B* lithology dependent constants. The parameter *A* represents the reciprocal of the thermal conductivity at T=0°C (cf. Table 1). The parameter *B*, which describes the decrease of λ with temperature, is also lithology dependent: samples of higher conductivity show a stronger temperature dependence than those with lower conductivity. On the basis of the data published by Clauser & Huenges (1995), *B* can be linearly interpolated between a maximum of $3.4 \cdot 10^{-4}$ W m^{-1} for $\lambda_{T=0°C} > 3.5$ W m^{-1}K^{-1} and a minimum of $3.2 \cdot 10^{-4}$ W m^{-1} for $\lambda_{T=0°C} < 2.5$ W m^{-1}K^{-1}. For temperatures above 450°C all thermal conductivity datasets occupy a very close bandwidth around 2 W m^{-1}K^{-1}. The pressure dependence is less pronounced: the increase of thermal conductivity with pressure can be as much as 15% at pressures of 10 MPa and stabilises at higher pressure regimes. The pressure correction used for this work involves a linear increase of thermal conductivity from 0 to 10% over the pressure range 0 to 10 MPa. Thereafter the conductivity remains independent of pressure.

Although anisotropy is not specially treated in this paper, it must be kept in mind that these relationships concern all components of a thermal conductivity tensor. The general tensorial form of thermal conductivity is the result of a transformation from a local, geologic coordinate system into the global coordinate system of the whole domain under consideration. However, in the case of isotropic materials the thermal conductivity can be treated in scalar form since the transformed structure will again be isotropic.

The rate of heat production depends mainly on the U, Th and K contents. Therefore, granitic lithologies produce more heat than sediments (see e.g. Rybach, 1988). U, Th and K are preferentially enriched in the upper crust. The depth profiles of heat production assume an exponential decrease in the mid and lower crust.

4 NUMERICAL AND DISCRETISATION PROCEDURE

The simulation tool is the three-dimensional finite element code FRACTure (Kohl et al., 1993). Among other features, the program allows steady state and transient simulations of the coupled hydraulic and thermal processes in the underground. Special emphasis is given to treat the non-linear temperature and pressure dependence of thermal conductivity. This property is adjusted according to the local temperature and pressure field by the lithology-specific functions mentioned above. Since FRACTure uses a linear solution algorithm, the solution will be approached by iteration. For the type of problems discussed convergence is reached typically within 10 iterations.

Special emphasis is devoted to the discretisation of irregular finite element networks. Experience shows that automatic mesh generation of arbitrarily shaped bodies nearly always needs successive manual adjustment. Therefore, a special module for the mesh generating code FRAM was designed. To treat a given domain, a rough finite element mesh is first discretised manually using all advantages of a commercial CAD software package. In a second step the code refines the mesh automatically. The possibility for insertion of a scanned geologic section into the CAD software to give a background pattern for the discretisation is a further convenient feature. Copying these two-dimensional discretisations into the third dimension and applying the appropriate material properties yields a full three-dimensional mesh. Additional tools incorporated in FRAM allow the rotation of these three-dimensional bodies or the selection of optional cross-sections which can be transposed. The latter option also permits the upper surface of a body, to be adjusted to the true topography, or the shape of an irregular internal geologic layer to be represented.

5 SIMULATION OF THE UPPER PART OF KTB-VB

5.1 Background and preparatory investigations

The aim of the simulation of the upper 2000 m of the VB was to elucidate the three-dimensional thermo-hydraulic effects in this zone. This was possible since the VB database is more complete and reliable than the HB database. The thermal effects caused by the strong lateral heterogeneities in the vicinity of the KTB site require considerations in a depth range in which three-dimensional information is available. This is generally the uppermost part of a borehole since surface considerations can add information from the two horizontal dimensions to the one-dimensional borehole information. The topography-driven hydraulic flow field and the steeply dipping gneissic and metabasitic structures represent first order lateral heterogeneities. Necessary information on the adjacent geologic structures is available from the analysis of core samples and the distribution of geologic units on the surface. The characterisation of the hydraulic influence on the thermal field requires a special approach since the relevant local hydraulic regime needs to be determined.

Before modelling the thermal regime near the surface, the distribution of thermal conductivity and heat production for the different lithologies were evaluated. On one hand the data collection of the KTB field laboratory could be used but on the other hand also the surrounding materials like granite, graphitic quartzite and greenstones had to be investigated. Therefore, near surface materials were collected and their thermal conductivity was measured (Medici, 1994; unpublished). Astonishingly high thermal conductivity (higher than 7 W m^{-1}K^{-1}) was determined for the graphitic layers of the Wetzldorf sequence located 5 km northward of the KTB which agrees well with the findings of Jobmann & Clauser (1994). This unit represents the collision zone between the Moldanubicum and the Saxothuringian that was originally targeted to be drilled in the KTB project. This sequence extends laterally only 3 km in E-W direction at the surface and has a rather limited thickness. Since it is uncertain whether the graphitic quartzites extend further down to greater depths they were not considered in the present study.

The model consists of the following materials: Sediments, metabasite, gneiss and granite. Although known to be anisotropic, the thermal conductivity of the steeply dipping gneissic formations was treated as isotropic. The value of the thermal conductivity was chosen to be the vertical component originating from the mean dip of gneiss. The diffusive thermal material parameters at reference temperature of 20°C and zero pressure of the four materials (sediments, metabasite, intermediate dipping gneiss and granite) used in the 3-D model are shown in Table 1.

Since the objective of the thermal simulation was to explain the measured temperature field by the thermal conductivity and heat production structure, the measured values of these parameters were left unchanged. This represents a strong restriction for the fitting procedure, since the measured temperature data should be

explainable by two homogeneous materials only (metabasite and steeply dipping gneiss) that were encountered in the KTB.

Table 1. Thermal material properties (at 20°C) for 2-D / 3-D simulation

	thermal conductivity [W $m^{-1}K^{-1}$]	heat production [μW m^{-3}]
sediments	2.0	0.4
gneiss, steep	3.3	1.5
gneiss, intermediate	3.2	1.5
gneiss, near-horizontal	3.0	1.5
metabasite	2.5	0.8
granite	3.7	6.0
mid crustal	3.4	1.0 - 0.6

Our sequential approach in modelling will be as follows: a regional hydraulic model to define the lateral borders of a refined 3-D model, a local thermal model to investigate a thermal diffusive field and finally a local thermo-hydraulic model for the evaluation of advective thermal transport.

5.2 3-D regional hydraulic model and model definition

The evaluation of the local hydraulic regime requires a model with reliably known lateral boundary conditions. Therefore, a large regional three-dimensional model was set-up extending laterally over the surface indicated by Fig. 1 and from which a local model was extracted. Furthermore a refined accurate thermal transport calculation can be only performed on a smaller model. The detailed study on the thermal and hydraulic field at the KTB site which was performed on this second, smaller block model is described in chapters 5.3 and 5.4.

The following topographic features define the lateral boundaries of the regional model that incorporates possible hydraulic sinks and sources at a large distance from the KTB: the 900 m high southern foothills of the Fichtelgebirge approx. 13 km north of KTB, the lower plains (430 m altitude) until a distance of 28 km west of KTB, the undulating 550 m high hills 10 km east of KTB and the conjunction of Haidennaab and Waldnaab Rivers 20 km south of KTB. The digitised topographic data were supplied by the Bavarian Geodetic Survey (Bayrisches Landesvermessungsamt, 1994) on a 200m x 200m mesh.

As a first order assumption the hydraulic head was taken at topographic height. Numerous lakes justify this approximation since they indicate the water level to be close to the surface. The preliminary interpretations of Kessels et al. (1992) that propound a hydraulic pressure field at around 2000 m decoupled from near surface influence together with the observation of a strong heat flow contrast in the uppermost 2000 m suggests a no-flow boundary for the topography driven, regional flow field at a depth of 3500 m. The same boundary conditions were taken for all lateral boundaries. Thus, this model assumes no topography-driven fluid flow below the 3500 m depth boundary and a negligible influence of the lateral boundaries at a distance of minimum 10 km on the head distribution near the KTB. The lateral discretisation took into account the topographic structures like valleys and mountains, and as well as the permeability change between crystalline and sedimentary units. The model was discretised into 9000 nodes and 8900 prism elements with a quadrilateral or triangular cross-sections and linear shape functions. Fig. 3 shows the mesh in a perspective view.

The results of a series of runs performed with a representative model differentiating between crystalline units of low permeability (10^{-18} m^2) and permeable (10^{-16} m^2) sedimentary units are given in Fig. 4 which shows the variation of the hydraulic field with depth. Close to the surface a rather dispersed flow pattern can be recognised. This tends towards a N-S directed flow at greater depth. The differences in the head distribution decrease with depth, resulting in the strongest flows in the near surface layers. The mountains of the southern Fichtelgebirge and the lows of the southern valleys dominate the hydraulic behaviour. The flow field at the Frankonian Lineament which represents an impressive, well visible surface structure and separates the sedimentary units in the west from the crystalline block is not connected to the KTB site. This contrasts with the 2-D models of Clauser & Huenges (1993) or Jobmann & Clauser (1994). The local flow field in the vicinity of KTB is mostly influenced by the nearby valley of the Fichtelnaab River.

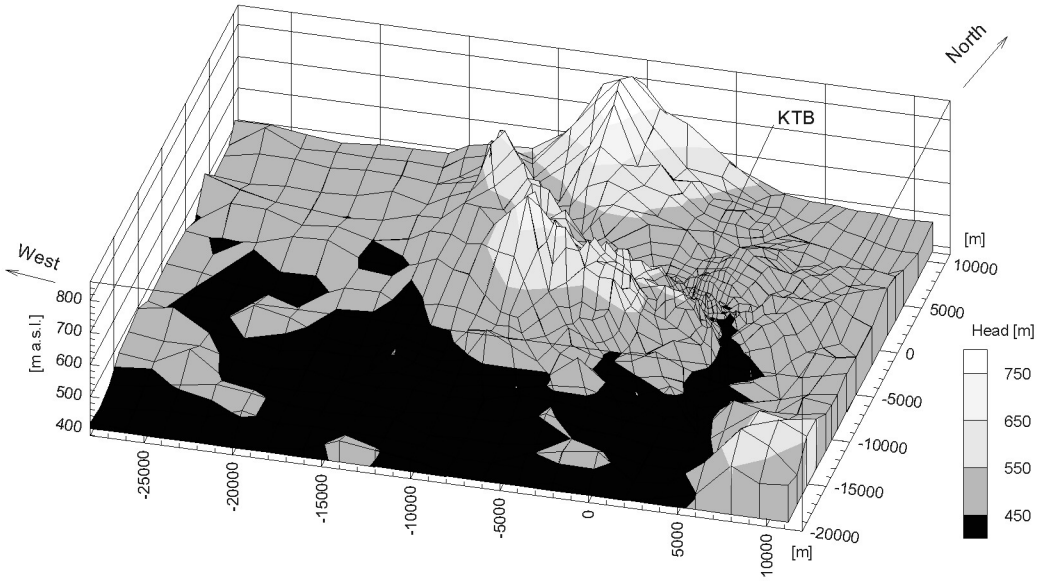

Figure 3. Finite element discretisation, elevation and surface head distribution of the 3-D regional model. The mesh follows the topographical units and is most refined in the vicinity of the KTB (at 0,0,505).

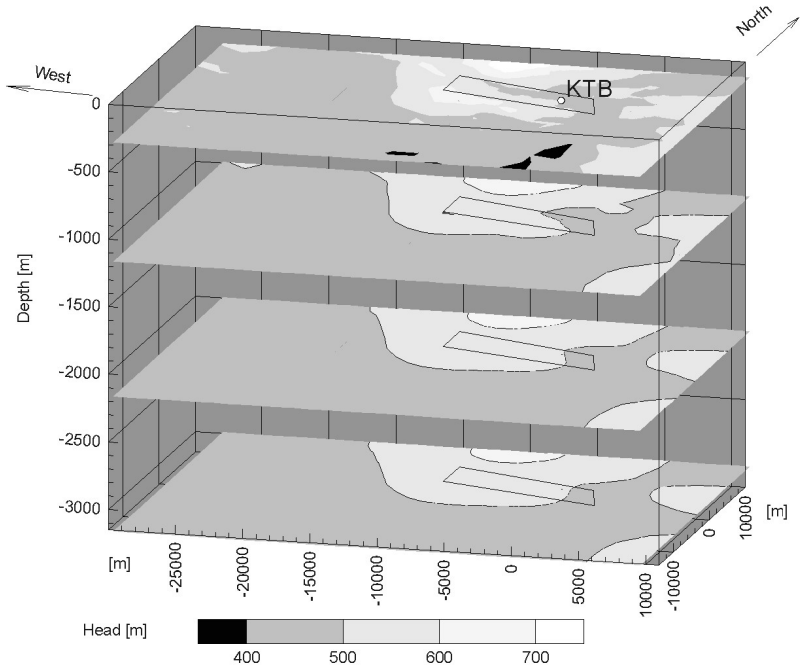

Figure 4. Three-dimensional regional hydraulic situation. The black lines indicate the boundaries of the smaller block extracted for the local model. It is to be noted that the KTB is not located in the centre of the small block.

A reduction of the lateral block size of this regional model to create a more detailed local model can only be made if there are no significant horizontal components of hydraulic flow at the lateral boundaries of the smaller model. The definition of such Neumann type boundary condition for the hydraulic field can only be performed on ridges or on deep valleys. Fortunately, a central zone could be found (indicated by black lines in Fig. 4)

that fulfils this requirement. This zone is bounded by the Fichtelnaab River in the north and the Waldnaab River in the east, by the nearly 700 m high altitudes in the west and S-W (Kühberg) and by the N-E dipping slope of the hills south of the KTB. In contrast to the hydraulic flow field with its dominating horizontal components, the thermal heat flow field is directed nearly vertically upwards. Thus, the model with a nearest boundary at 2 km distance to the KTB-VB does not influence the thermal field at the VB.

Due to the topographic constraints the local model's shape is not rectangular. The model extends in E-W direction over 10 km, in N-S direction from 3 km at the eastern border to 7 km at the western border. The northern boundary is located closely to the KTB (about 2 km).

The advantage of a smaller block model is obvious: due to computer storage restrictions the large regional model could not be discretised finely enough. The small model however, uses elements with a length of 50 m in the vicinity of KTB. Thus, structural constraints from surface or borehole geology (fracture zones, small lithological heterogeneities) could be taken into account. At larger lateral distance the mesh becomes coarser with lateral element lengths up to 500 m. The total domain contains four different geologic units: Cretaceous sediments in the west, granite in the north-east and gneiss and metabasite in the central region. A perspective view of this model is displayed in Fig. 5. The final model contained 8000 linear elements with a total of 9000 nodes.

The following procedure was chosen for assigning the material distribution to the model: The large geologic structures at the surface like metabasite, (steep) gneiss and granite were projected into the subsurface. A fit of the measured dataset required a variation of the geologic units with depth. With the exception of the granitic intrusion where a terminal depth the properties of the metabasitic or of the gneissic block were allowed to vary with depth. The depth of that small part of the large granitic intrusion NE of KTB which falls within the model geometry was taken to be 2000 m in agreement to the Hirschmann (1993) interpretation. The only depth information available is represented by the KTB-VB profile. The KTB-VB site is defined by a vertical column with 100 m x 100 m cross-section that contains the measured borehole profile. The material properties of this column, which correspond to the measured dataset, remained unchanged during the modelling process. Furthermore, the steeply dipping, 400 m wide Nottersdorf Fault Zone (Hirschmann, 1992; see also Fig. 6) was especially investigated, since it likely represents an important tectonic unit for the uppermost temperature field. An enlargement of the surface material distribution in the vicinity of KTB-VB that contains these five units (gneiss, metabasite, granite, KTB-VB site and Nottersdorf Fault zone) is shown in Fig. 6.

The next section describes a thermal diffusive simulation on this second model. Based on varying permeability assumptions a refined hydraulic field will be evaluated and quantified for its thermal implications in a later step.

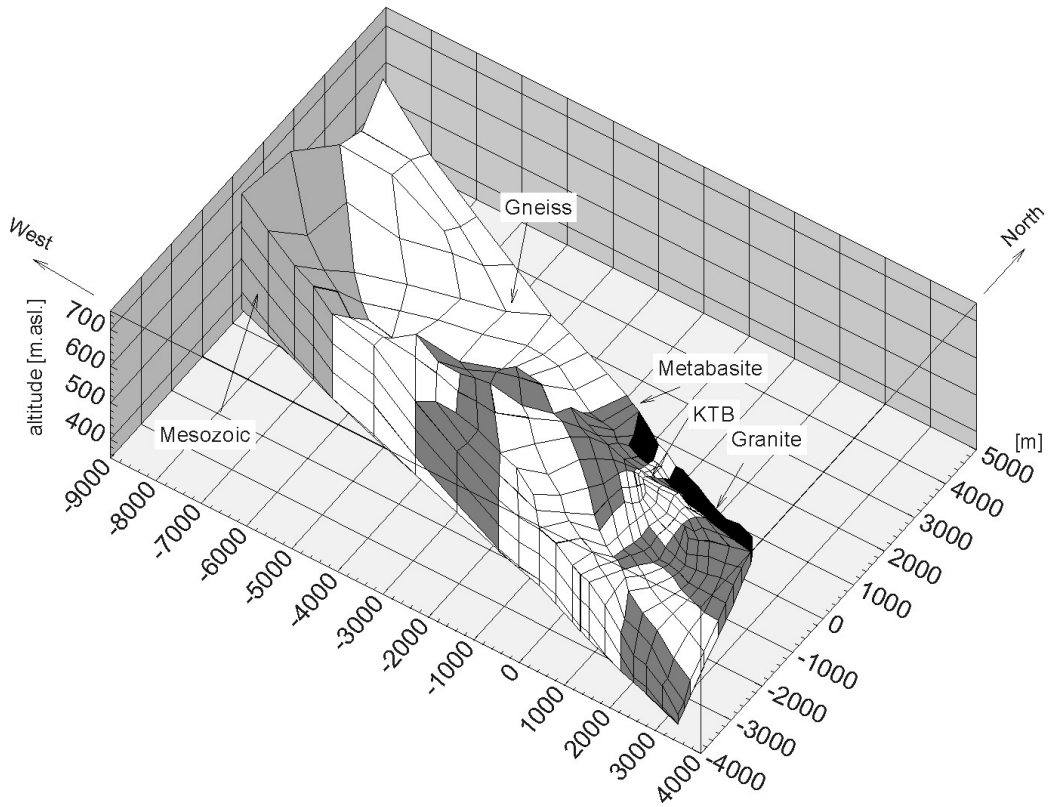

Figure 5. Perspectivic view on the local 3-D thermo-hydraulic model. The figure represents topographic heights, geological units and discretisation between surface and 350 m. In the x/y plane, the Kühberg is located near the coordinates (-7000,0).

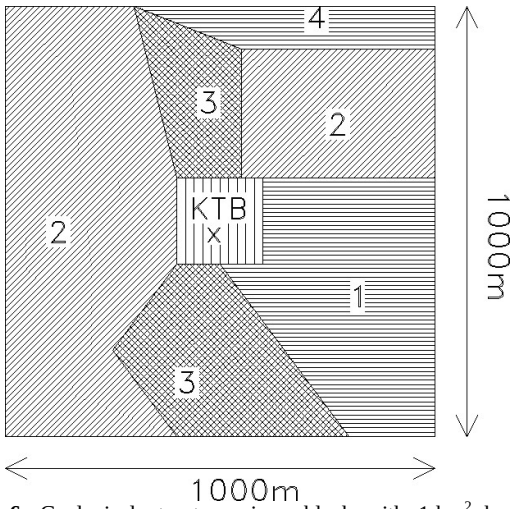

Figure 6. Geological structures in a block with 1 km^2 horizontal cross-section around the KTB. At the surface, the domains 1 and 3 correlate to gneiss, domain 2 to metabasite and domain 4 to granite. The domain 3 represents the Nottersdorf Fault Zone. KTB represents the VB location.

5.3 3-D thermal model

First efforts at thermal modelling concentrated on describing the measured temperature profile by purely diffusive assumptions. Since the foliation of the gneissic and metabasitic structures is very steep, abrupt lateral changes of the adjacent material are likely. Locally, at the KTB site, material changes (i.e. changes from gneissic to metabasitic structures) were allowed for each of the three adjacent domains (granitic intrusion remained fixed) as illustrated in Fig. 6. However, this procedure still imposes strong restrictions on a data fit:

- The chosen geometry remained unchanged: Since the central KTB domain has a lateral cross-section of 100 m x 100 m, a lateral effect has to extend over a minimum distance of 50 m.
- The only materials to be interchanged laterally were gneiss and metabasite. Although the fitting process allows for a complex lateral geometry, the simplest distribution model (consisting of the mean gneissic and metabasitic properties) in the domains adjacent to the KTB was assumed.

An altitude dependent surface temperature with a free air gradient of 0.004 K m^{-1} was taken. The extrapolation of the VB temperature log results in a surface temperature of 8.5°C, BHT measurements indicate 7.4°C at the surface. Therefore, the ground surface temperature was fixed at the KTB with 8°C. A measured temperature value was taken as the lower boundary temperature of the model (103°C at 3500 m). No lateral heat flow was assumed at the lateral boundaries. Thus, the lower boundary is sufficiently far away from the uppermost 2000 m depth section considered here. Since the VB provided reasonably good temperature logs and excellent thermal conductivity core measurements the thermal model will only be compared to the VB data. Necessary criteria for the model are a satisfactory fit of the measured temperature and temperature gradient. Since the thermal property of the KTB remained fixed and were taken from core measurements a fit of the temperature gradient automatically provides a good heat flow fit.

The best fit was achieved with model run D03a (Figs. 7, 8). The constraints of this model will be discussed only for a block with a 1 km^2 cross-section around the KTB. For the purpose of our overview attempt this block characterises best all the three-dimensional implications on the temperature field. In Fig. 7 the material distribution, the temperature gradient and the heat flow are illustrated for this block. A somewhat extreme property distribution had to be chosen to fit the temperature profile. Especially for the thermal conductivity between 1800 and 2400 m a model had to be chosen that assumes a small, isolated gneissic body, surrounded by metabasitic complexes. The lithology in the 200 m distant HB drillhole, where only metabasite was encountered in this depth range can support this assumption.

The model suggests two different sections with a continuous transition in between. The uppermost depth section down to 1200 m is dominated by the gneissic influence. This can also be substantiated by surface geology and the VB profile, where gneiss was encountered between 500 m and 1200 m. Our model predicts in this section about 75% gneissic material and 25% metabasite. This is in good agreement with the material distribution known from the surface that shows 65% gneissic or granitic and only 35% of metabasitic material. The second depth section between 1200 m and 2500 m is mainly dominated by metabasite. In the vicinity of the KTB, the best fit model requires about 80% metabasite and only 20% gneiss. This material distribution does not reflect however the characteristics of the cored material which consists mainly of gneiss. Such results suggest a "chimney" effect with heat preferentially flowing along the well conducting, small-size gneissic rock masses. A predominantly metabasitic portion of the surrounding rock masses can explain the high vertical gradient zones that were measured in the gneissic part of the VB profile at about 2000 m depth.

Fig. 8 compares the three measured VB observables thermal conductivity (vertical component), temperature and vertical temperature gradient (averaged over the approximate mesh size of 100 m) to a 1-D profile extracted from model D03a. With the exception of the uppermost 200 m a good data fit was achieved. The characteristic decrease in the reduced temperature representation (on the basis of a mean gradient of 0.028 K m^{-1}) cannot be completely simulated, a maximum deviation of 1°C still remains between the logs and the model. The same applies to the vertical temperature gradient, where deviations of 0.002 K m^{-1} are apparent. The undulations of the temperature gradient with the strongest variation in the uppermost 200 m (on the order of 0.007 K m^{-1}) cannot be simulated by this model.

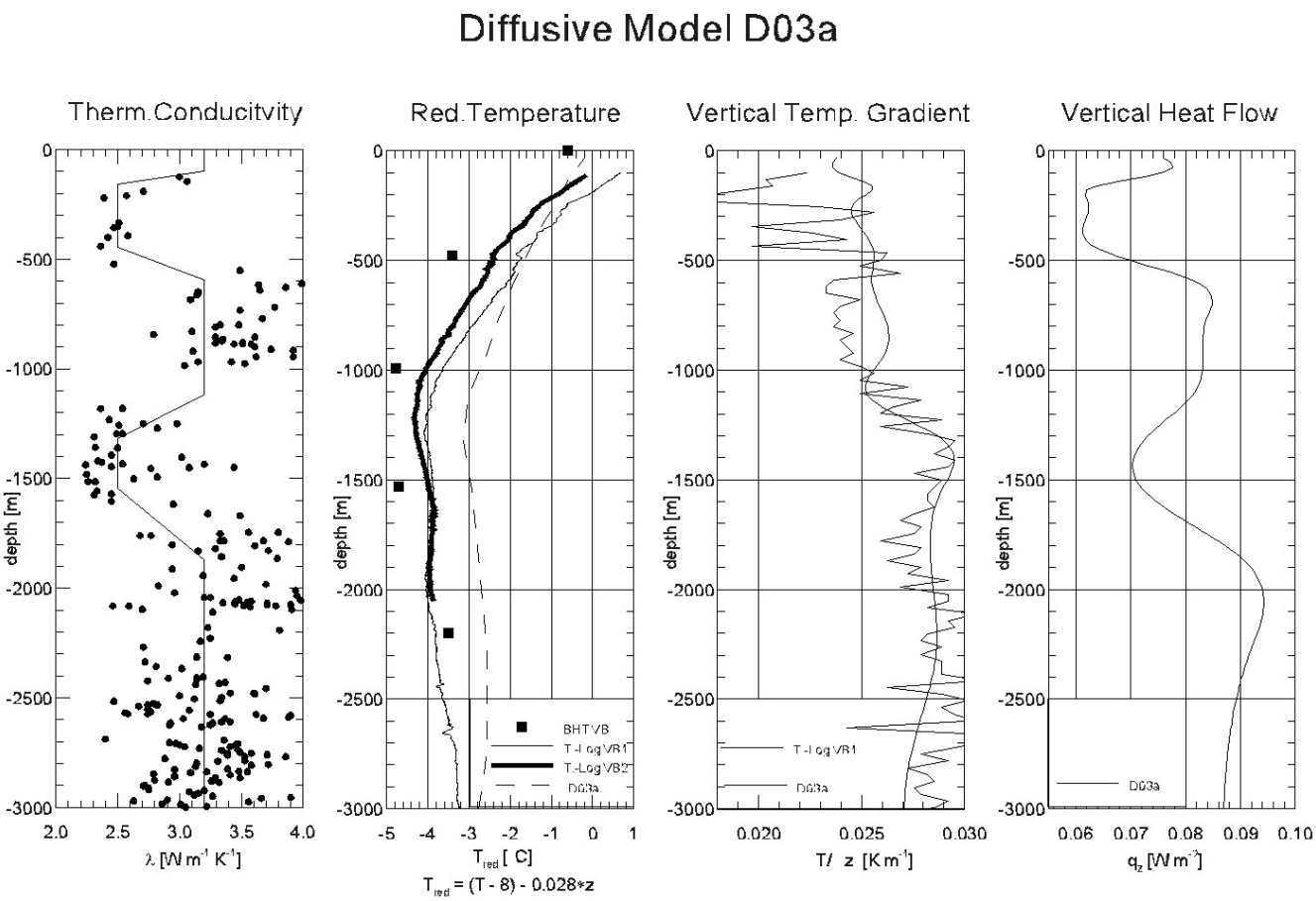

Figure 8. 1-D profiles showing the geothermal situation along the KTB - VB profile. The plot at the extreme left shows the thermal conductivity distribution (dots represent the vertical component of VB core measurements and the straight line represent model D03a). The next graph to the right (reduced temperature) shows the two measured temperature logs in the VB as well as the result of model D03a (thick dashed line). The third graph compares the measured and the modelled (thick line) temperature gradient. Finally, the graph at the extreme right shows the apparent vertical heat flow profile in the VB borehole.

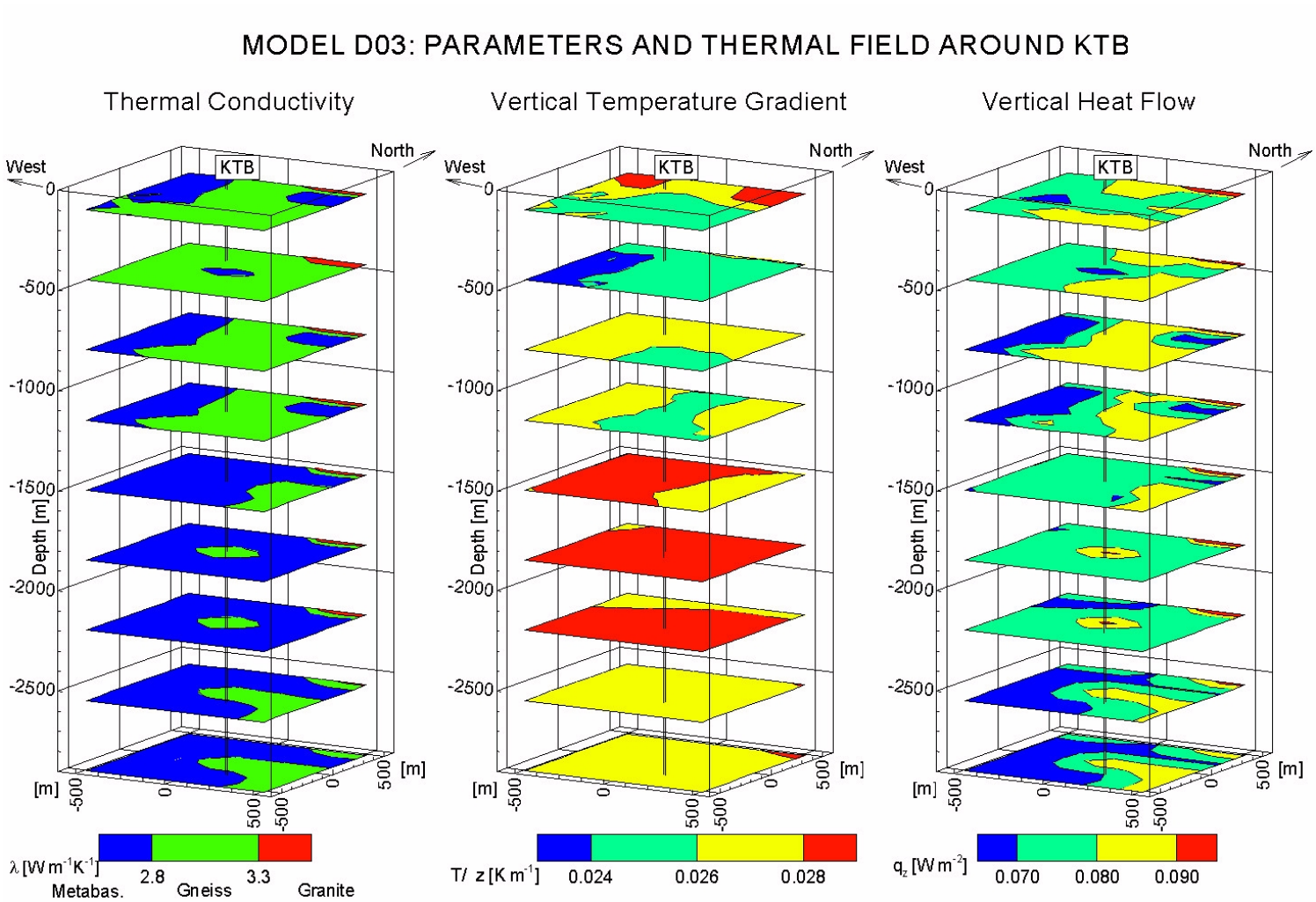

Figure 7. Block diagrams showing the thermal input parameters and the calculated thermal field in the vicinity of KTB for the purely diffusive model D03a. To the left, the distribution of gneiss, metabasite and granite (the very North East) can be recognised. The illustration in the middle shows the vertical temperature gradient distribution and the rightmost illustration the corresponding effects on the vertical heat flow.

Adapted from *Geophys. J. Int.*, **124**, *756-776*

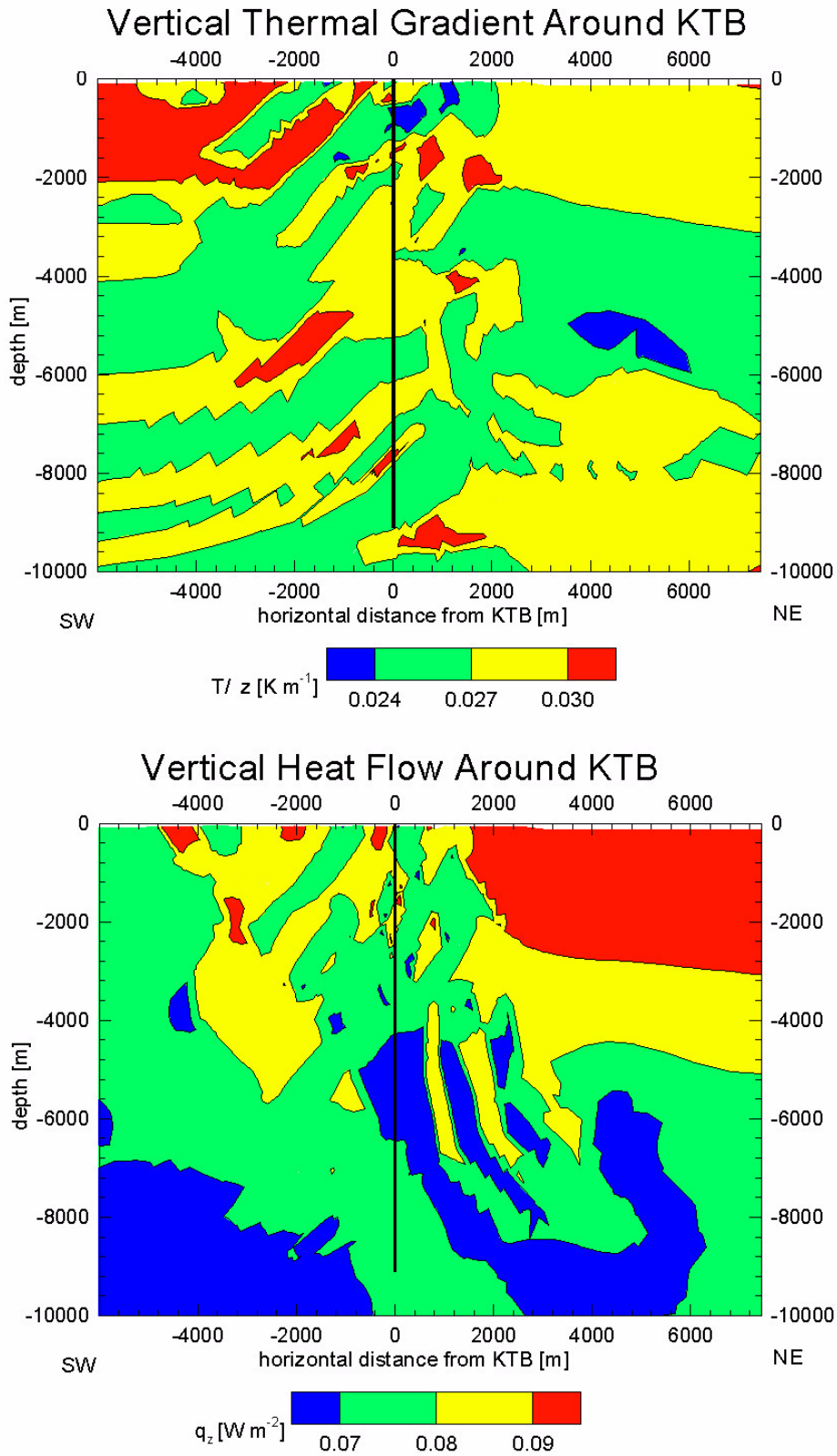

Figure 13. Distribution of the vertical thermal gradient (top) and the vertical heat flow component (bottom) for the diffusive model of the upper crust. Note that the isolines indicate a 12% variation from the mean value in both plots. This model excludes near surface effects of the low heat flow zone. The black vertical line represents the KTB.

Unfortunately, the uppermost 200 m are not very well documented by the field measurements and therefore do not constrain well model D03a (only 3 thermal conductivity measurements down to 200 m are available - see also Bücker et al., 1990). For an explanation of this feature further heat flow mechanisms can be considered. Due to the abrupt changes, these small size effects seem to indicate advective thermal transport rather than paleoclimatic influence.

In summarising these results, we see that a three-dimensional thermal diffusive model is able to explain the presence of a low heat flow zone in the upper 500 m, discussed in chapter 2. The non-satisfactory fit of the uppermost 200 m may be improved by assuming advective thermal transport.

5.4 3-D local hydraulic model

The influence of advective heat transport on the temperature field can only be assessed by using geometrically simple models. It is clear that such basic models will not represent perfectly the hydraulic behaviour in the crystalline subsurface. High permeability zones will rather show up as distinct hydraulic effects on the thermal field. Lack of data for a sophisticated hydraulic simulation has lead to the investigation of three alternative hydrogeologic assumptions:

- 3500 m (deep) homogeneous permeability (run "d"): General hydraulic behaviour is highlighted by a flow circulation down to a depth of 3500 m.
- 500 m (shallow) homogeneous permeability (run "e"): This model characterises shallow flow circulation, limited to a depth of 500 m
- Nottersdorf Fault assumption (run "f"): This model contains the hydraulically most active structure with an assumed model depth of 800 m .

These three models are summarised in Table 2. The effects of the three assumptions on the thermal model D03a are then needed, together with the measured temperature data to evaluate the necessary permeability distribution.

The calculations performed on homogeneous model (run "d") will be described more in detail, because they illustrate very clearly the hydraulic impact. Astonishing effects are revealed:

The SW-NE flow in this model has a direction nearly opposite to the overall regional trend (from north to south). From 200 m downward, rising fluids have to be expected near the vertical KTB profile. In the fence diagram of Fig. 9 the pattern of downwards fluid migration due to the presence of the hills in the west (Fig. 5) can be recognised. The local hydraulic low which is represented by the Fichtelnaab Valley (Fig. 1) is of rather small dimension (width 100 - 200 m). Therefore the deeper fluids start rising before reaching the KTB site, whereas the near surface fluids are still percolating downward. For a given permeability of $2x10^{-15}$ m^2 the equilibrium between downward and upward percolating fluids at the KTB location is attained at a depth of about 200 m.

Table 2. Description and parameters of hydraulic models

	description	high permeable structure	low permeable structure
run "d"	homogeneous	$2{\cdot}10^{-15}m^2$	$2{\cdot}10^{-15}m^2$
run "e"	2 horizontal layers	uppermost 500 m; $10^{-15}m^2$	bedrock; $<10^{-18}m^2$
run "f"	Nottersdorf-Fault (N-S)	400 m lat., 800 m vert. Extension; $2{\cdot}10^{-15}m^2$	surrounding rock $<10^{-18}m^2$

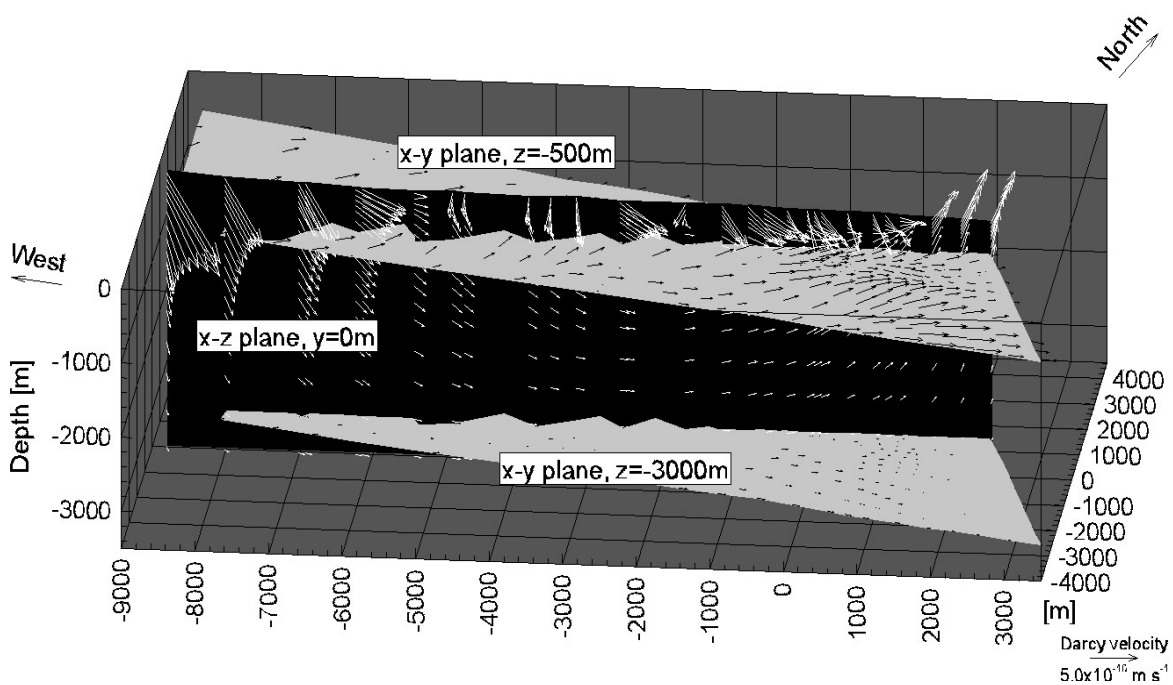

Figure 9. The local hydraulic flow field for a hypothetical uniform permeability of $10^{-15}m^2$. The KTB is located at x/y=0/0. The vertical flow field in the east-west direction through the KTB (i.e. *x-z* plane) is indicated by white arrows, the horizontal flow field at depths z=-500 m and z=-3000 m (i.e. *x-y* planes) is indicated by black arrows. The flow field at the KTB below 200 m is upwards and above 200 m downwards directed.

High permeabilities are required to create a sensible thermal effect. Only permeabilities greater than 10^{-15} m^2 show a clear, characteristic hydraulic impact on the thermal field. This high value is necessary to allow sufficient fluid flow under the driving influence of the low mean head gradient on the surface from the Kühberg to the Fichtelnaab Valley (~0.03) and due to the rotation of the main drainage axis from the 120°N strike of the Fichtelnaab to the 180°N strike of the Waldnaab. This directional change causes a convex, diverging flow pattern and thereby tends to reduce the flow intensity.

The implications on temperature and temperature gradient of all three models are shown quantitatively in Fig. 10. A uniform permeability of $2{\cdot}10^{-15}$ m^2 for the 3500 m deep model was chosen, which is one magnitude above the highest measured permeabilities. Upwards fluid motion at greater depths will cause a heating of the subsurface below the KTB location. Since a Neumann type hydraulic boundary condition and a fixed temperature boundary condition were applied at the base of the model, the rising fluids yield a maximum deviation of the temperature from the diffusive model at 1200 m (~1/3 of the model depth). Models which assume lower boundaries deeper than 3500 m will show similar effects: the temperature difference between the thermo-hydraulic and the purely diffusive models will increase to a maximum at a characteristic depth and decrease thereafter. Thus, from a thermal point of view, deep circulation / high permeability flow models for the KTB site can be discarded since the upwards directed flow pattern would lead to lower gradients at greater depths ranges and higher gradients at shallower depth, an effect opposite to the measured thermal profiles.

The second alternative model, assuming shallower flow down to 500 m depth leads to a different thermal effect. Infiltrating from the cool surface, the fluids percolate downward in the subsurface. The cooling effect dominates. Model "e" shows the thermal impacts for this shallow model that assumes a uniform permeability of 10^{-15} m^2 for the uppermost 500 m and 10^{-18} m^2 for the region below. It is obvious that only the uppermost depth range is affected by the circulation. A further sophistication of this approach is potentially able to explain the low temperature gradient in this upper section.

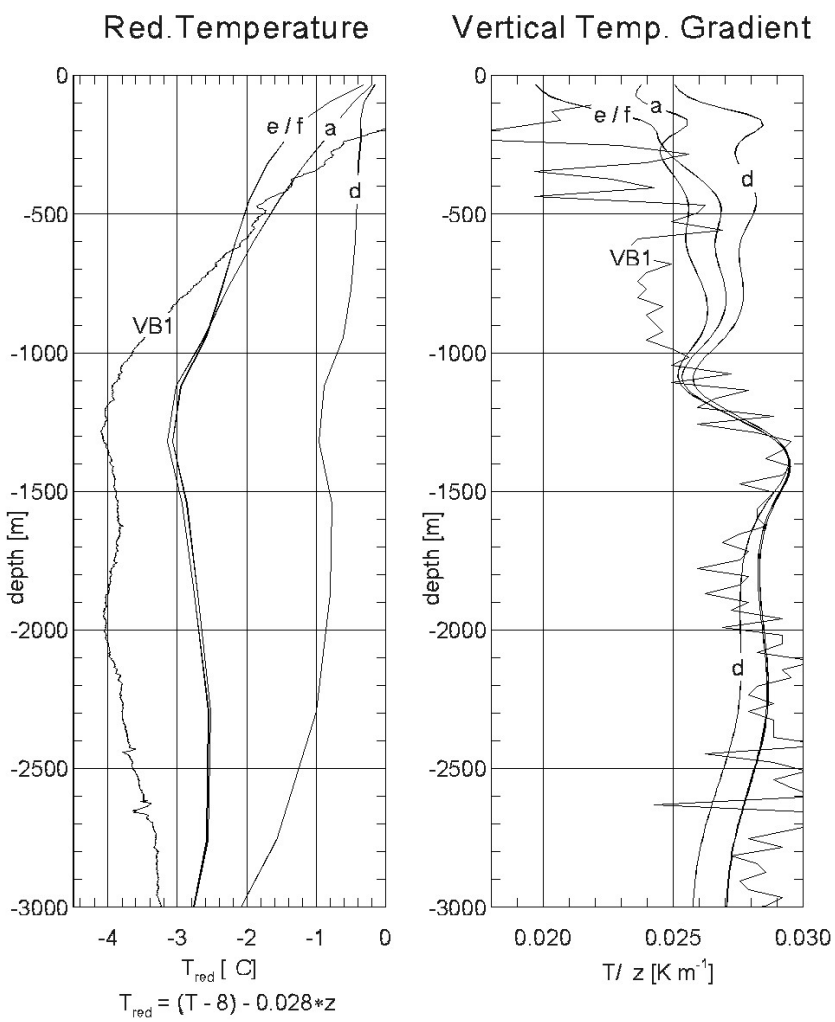

Figure 10. 1-D profiles showing the influence on reduced temperature and temperature gradient of two different hydraulic models. Model run "d" represents the result of a homogeneous permeability distribution, run "e" represents the result of a homogeneous permeability at shallow depth, run "f" represents the Nottersdorf - Fault case. The curves of run "e" and "f" are nearly identical. Additionally, the diffusive model D03a ("a") and the first VB temperature log ("VB1") are plotted.

However, another approach seems indispensable since the hydraulically active fractures in the uppermost 800 m section of the VB can all be related to the Nottersdorf Fault zone (Hirschmann, 1992). Close to the KTB the 400 m broad, 160°N striking and 60° to 90° eastward dipping Nottersdorf Fault Zone is situated. The surface outcrops of this fault zone range from 560 m down to 440 m elevation at the Fichtelnaab River. The neighbourhood of the Nottersdorf-Fault Zone down to 800 m depth is likely to be characterised by a higher permeability than the surrounding materials. Thus, it may strongly influence the flow field near the KTB.

An effective thermal transport by the Nottersdorf Fault model (run "f") requires high permeabilities, too. These are due to the even smaller head gradient on the surface (0.02) since the 160° striking profile of the fault zone is not oriented parallel with the steepest surface inclination. For model "f" a permeability of $2x10^{-15}$ m^2 for the Nottersdorf Fault down to 800 m depth and 10^{-18} m^2 for the surrounding rock masses is assumed. Like run "e", this model yields a strong decrease of the thermal gradient in the upper 150 m. The temperature field in the deeper section that is well represented by the diffusive model D03a (run "a" in Fig. 10) is only slightly affected.

It is evident that three-dimensional considerations are indispensable for the evaluation of the local hydraulic flow regime, since the meso-scale variations of topographic height around the KTB site cause a complex flow pattern in the subsurface. A three-dimensional flow analysis reveals only rarely a planar two-dimensional flow but more often a convex, diverging (like at the KTB site) or concave, converging flow pattern. Models that contain a rather complex thermal conductivity distribution and assumptions on permeabilities which restrict hydraulic flow to shallow depth are well suited to describe the measured temperature profile in the upper 200 m of the KTB site. The hydraulic considerations are confirmed by Jobmann (1990) and Stiefel (1990) who have detected hydraulically active fracture zones in the upper part of the VB that are located at 300 m, 500 m and 600 m depth. A topographically driven hydraulic flow field can only be inferred for the uppermost section of the drilled depth. Our considerations strongly suggest purely diffusive thermal transport for the main part of the drilled KTB depth range. A different model assumption led Jobmann & Clauser (1994) to a similar conclusion.

For various reasons drill sites are often situated on high ground. The KTB site follows this pattern. In a terrain with high permeability at shallow depth, a drill hole at such sites is likely to be exposed to downwards percolating fluids. This mechanisms could be responsible for the erroneous temperature prediction during the site investigation study (see for example the location of drillhole Püllersreuth and Rummelsberg on Fig. 1; cf. Burkhardt et al., 1989).

6 THERMAL SIMULATION OF DRILLED KTB-HB DEPTH

6.1 Geologic cross-section

This second simulation was aimed at the investigation of thermal effects along the drilled depth of the KTB-HB, i.e. the upper crust. It was intended to set up a thermal model for the KTB location containing the available geologic knowledge and accounting for realistic heat flow mechanisms. As shown above, no thermally significant fluid flow can be expected over most of the drilled depth.

The most complete geologic interpretation for the drilled KTB depth section is presented by Hirschmann (1993). It is based on direct borehole data, on geologic mapping and on geophysical surveys in the KTB region. He describes a SW-NE striking profile with strongly dipping gneissic and metabasitic structures at the ZEV. The region is bounded laterally by surface sediments to the SW and by granitic intrusions to the NE. The chosen SW-NE profile direction is parallel to the strike of the gneissic structures as observed in the borehole profile. The lack of information along the NW-SE direction (perpendicular to the Hirschmann profile) is obvious; however surface geology does not indicate any abrupt lithology change in the third dimension. Therefore, a two-dimensional approach to the greater part of the drilled depth down to 9 km seems to be appropriate. Fig. 11 shows the material distribution in the discretised domain. Clearly, the same features as on the Hirschmann profile are present: 60° dipping alternating lateral gneissic and metabasitic formations are situated in the centre of the ZEV near the KTB and at a lateral distance of 5 km horizontally layered units (near-horizontal gneiss) are encountered. Fig. 11 is slightly different from the Hirschmann profile since the model runs which fit the BHT measurements best require a lateral shift of up to 300 m of the surrounding geologic units.

Due to its greater depth range, the second model takes mid-crustal material into account as well. The choice of the mid-crustal material is not very critical with respect to thermal conductivity since its temperature dependence leads to a rather small bandwidth of variation, as discussed above. The thermal properties of the materials used for this 2-D simulation (sediments, near-horizontal gneiss, steeply dipping gneiss, granite, metabasite, mid-crustal material) are summarised in Table 1.

6.2 2-D thermal Model

In Fig. 12 the refined finite element mesh around the KTB is shown. This model consists of 3000 nodes. Different model runs have shown that finer spatial discretisation or the use of quadratic elements produces no significantly better results. For practical reasons it was decided to accelerate calculations by using the linear rather than the quadratic elements.

A mean annual surface temperature of 8°C was assumed as the upper boundary condition. The lower boundary was placed at a depth of 16000 m in the mid-crustal region, deep enough to have no effect at the depths range considered. Since neither the temperature field nor the heat flow is known for that depth, a plane of constant basal heat flow was assumed. The vertical heat flow at the lower boundary was varied in order to fit the measured temperature data. An optimum value of 0.063 W m^{-2} was found that corresponds to a temperature of 437°C at a depth of 16 km below the KTB.

The lateral boundaries are located at a distance of 6 km SW and 10 km NE of the KTB, where a vertical heat flow field is assumed. The distance is sufficient to leave the temperature field around the central area below the KTB uninfluenced by the boundary conditions. The simulation runs demonstrated that the lateral component of the heat flow vector is negligible except in the more steeply dipping gneissic zones where it reaches 10% of the total heat flow.

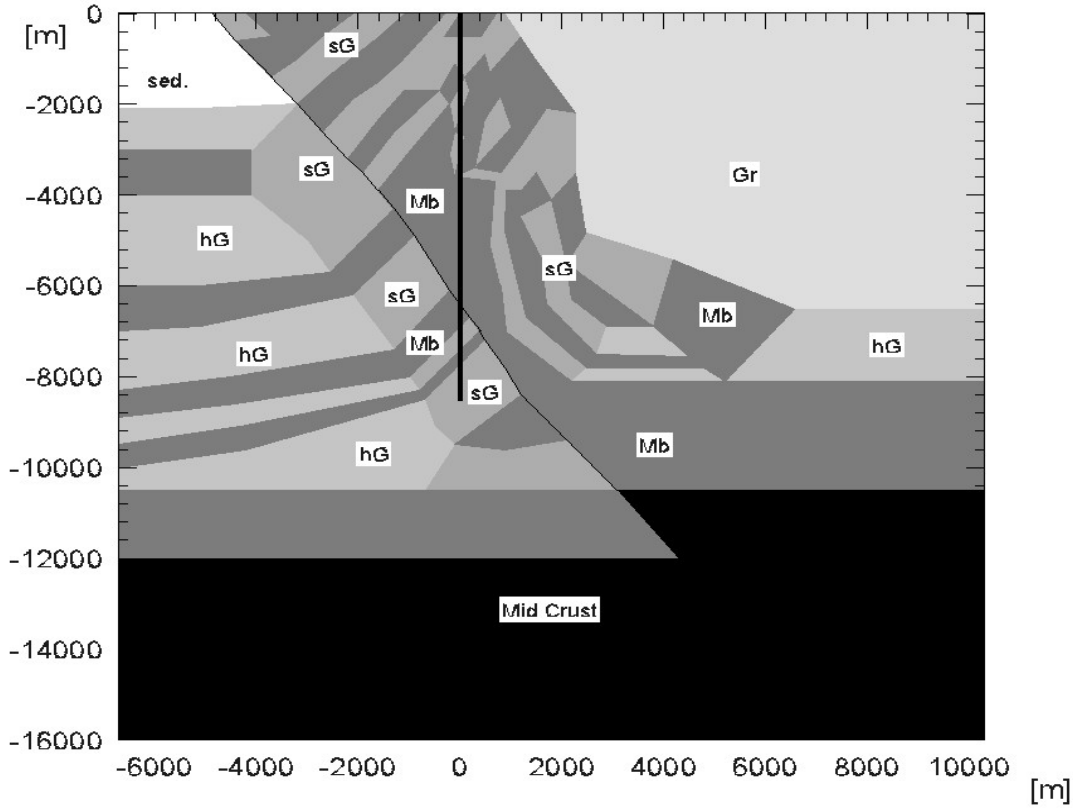

Figure 11. Material distribution of the discretised Hirschmann (1993) profile. The origin of the coordinate system corresponds to the borehole location on the surface. The black line represents the drillhole. Gr-granite, hG - near-horizontal gneiss, sG - steep gneiss and Mb - metabasite

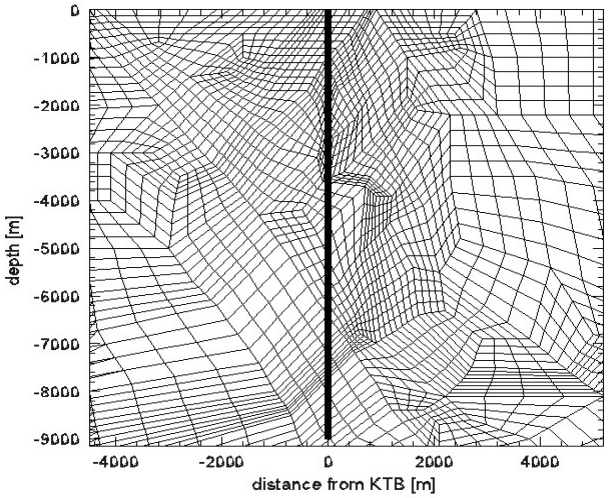

Figure 12. Detail of the finite element mesh in the near field around the KTB created by the mesh generator FRAM. The black line represents the drillhole down to a depth of 9000 m.

The available temperature logs only allow a comparison to the model in the VB depth section. The BHT values recorded during the HB phase can give punctual hints to the temperature profile but cannot be used to evaluate the temperature gradient. This represents the strongest restriction for the final evaluation of the model since we consider the thermal gradient as the most critical parameter for these steeply dipping zones (see later).

The results of the 2-D model will be discussed for the central ZEV region only, the peripheral regions of the model are rather subject to speculation. It must be pointed out also that deviations from the observed heat flow distribution must be expected for the uppermost 1000 m because it was not intended to optimise the uppermost heat flow zone using this diffusive model.

Fig. 13 shows the modelled depth distribution of the vertical components of thermal gradient and heat flow. In the vicinity of the KTB, a rather constant gradient accompanied by a stronger heat flow variation can be recognised. A comparison of the model profile to the available temperature data is given in Fig. 14. In the central part of the Hirschmann (1993) section the thermal behaviour can be described best if the material distribution of Fig. 11 is compared to the thermal gradient field in Fig. 13. A maximum variation of the thermal gradient on the order of 10% can be found that is by far lower than the 20% variation in thermal conductivity. The usual inverse correlation of thermal conductivity with gradient is found only in the horizontally layered materials close to the lateral boundaries. Different hypothetical observation boreholes in the heterogeneous central part of the model would not show a strong change in thermal gradient. This effect suggests that temperature logging performed in a hypothetical adjacent (~1km) borehole would not differ strongly from the KTB temperature measurements. The KTB HB and VB themselves (200 m apart) demonstrate this. The BHT measurements in the HB coincide well with the VB temperature profile (except for the two first BHT values, which probably are inexact since they were measured at large borehole diameter and

therefore submitted to borehole convection). This fact can be considered as justification of the fixed temperature boundary condition in the 3-D model from chapter 5.3.

Thus, the general pattern of a uniform gradient distribution observed along the entire drilled depth section can be explained. Apart from the upper 500 m, the observed temperature gradient can be well represented by the model profile (Fig. 14). The strongest deviations occur around 3200 m and 4000 m. The general diffusive character of the thermal transport in the crystalline domain is not thrown into question by these two deviations, because they coincide with fractured zones near large fluid reservoirs (Huenges, 1993). The importance of a local temperature perturbation due to these reservoirs can only be explained after further temperature logs are made, since due to their preferential uptake of drilling mud these zones are most affected by the drilling process.

However, the heat flow variation in the central domain is stronger than the variation in temperature gradient (Fig. 13 bottom). As expected, heat flows preferentially along the steeply dipping gneissic units. Small (500 m) lithology variations in the subsurface result in a strong change. Near the lateral boundaries, the heat flow shows the uniform behaviour expected in horizontally layered materials. The area around the drill hole at about 6 km depth indicates that the lateral extension of such a heat flow anomaly extends even more than 500 m into the metabasite. On the other hand, sensitivity analysis performed on different conductivity values has demonstrated that the borehole profile is completely unaffected by the choice of granitic or of sedimentary material properties. The effect of strongly decreasing heat flow in the granitic area is due to the effect of decreasing thermal conductivity with depth as well as to the high heat production.

Fig. 14 shows the results of our model along the drilled section, down to the depth of 10 km. Also plotted are the measured observables thermal conductivity, temperature and vertical temperature gradient (averaged over the approximate mesh size of 100 m) which are available from cuttings and logs. The deviations between the model and the BHT values are within a bandwidth of 2 K. This must be considered as satisfactory in the light of the uncertainties in the data itself. The BHT values and temperature logs in the VB vary relatively to each other by as much as ±2 K. Thus, the data available for the HB does not allow a further refinement of the model at this stage.

7 SUMMARY ON THERMAL EFFECTS IN DIPPING LAYERS

It has been demonstrated that the available borehole temperature data and geologic inference provide the basis for an unambiguous geothermal interpretation of the upper crust by thermal diffusion at the KTB site. In steeply dipping zones with alternating thermal conductivity distribution, the analysis of the heat flow alone might lead to erroneous results. In ground water flow analysis this represents a commonly known effect (Freeze & Cherry, 1979). By demanding continuity for the flow component normal to the interface, simple graphical construction of dipping flow lines penetrating into a horizontally layered different medium yields a refraction effect. The following two-dimensional example, calculated with FRACTure, has been chosen to illustrate this effect in the geothermal context.

Assume an infinite, layered underground consisting of two materials with the thermal conductivities λ_1 and λ_2. Heat flows vertically and uniformly in the subsurface; heat production is ignored. The interface between the two materials is rotated about the coordinate origin (0,0) to dip between 0° (horizontally layered) and 80° (nearly vertical). A hypothetical vertical borehole penetrates the interface at the point (0,0). Fig. 15 characterises the temperature gradient and heat flow profiles, which would be encountered in this borehole. For a horizontally layered medium, the general pattern of uniform heat flow across the interface and a discontinuity in the temperature gradient at the interface are found. Successively increasing the dip angle results in the temperature gradient tending to become uniform and in the derived heat flow profile taking on a discontinuous form. The magnitude of the variation depends linearly on the initial values of λ_1 and λ_2 (in our calculation $\lambda_1 = 1.5 \cdot \lambda_2$ is assumed) and can therefore be easily derived for different conductivity ratios. A 90° dipping structure results finally in a vertical uniform mean gradient that takes into account the portion of the two adjacent materials.

The KTB seems to offer an excellent demonstration of the influence of lateral heterogeneities. Even under the assumption of a two-dimensional structure (Fig. 11) the 60° dipping units cause heat flow perturbations over a long distance (>1 km). Therefore the thermal field of Fig. 13 can be explained by applying the results of the example discussed above. In such steeply dipping structures it is suggested to speak of apparent vertical heat flow. Thus, it becomes evident that in steeply dipping structures it is not possible to apply a conventional interpretation of heat flow regimes derived from geothermal research in horizontally layered, sedimentary basins or simplified one-dimensional structures such as described for example by Chapman & Furlong (1992). The apparent heat flow is not easily interpretable since small lateral structural changes result in different heat flow values and might suggest (erroneously) further heat transport mechanisms. In such cases, the interpretation should focus on the temperature gradient. The magnitude of the gradient reflects the proportion of the adjacent materials. Ignoring the local conductivity measurements this simple 2-D model suggests that an inverse analysis can lead to an estimation of a mean thermal conductivity of the adjacent rock for 90° dipping interfaces, if assumptions on the mean heat flow field are available. The KTB datasets allow easily a comparison of the mean conductivities to the two cored materials gneiss and metabasite: A first order estimation (ignoring heat production, assuming 2-D, nearly subvertical structures) that assumes a mean heat flow of 0.075 W/m^2 and the temperature gradient between 400 m and 1100 m of 0.024 K/m yields a surrounding material with a mean thermal conductivity of 3.1 $W\,m^{-1}K^{-1}$. This value corresponds to a composition of 89% gneiss and 11% metabasite if the thermal conductivities of Table 1 for steeply dipping gneiss and metabasite are applied. A temperature gradient of 0.028 K/m measured below 1100 m yields 25% gneiss and 75% metabasite. A comparison with the results of the more sophisticated three-dimensional thermal model of chapter 5.3 shows rather small differences (D03a: 65%/35% and 20%/80% respectively). This demonstrates that a quantitative estimation of the relative portion of the surrounding gneissic and metabasitic material is possible even under the conditions of the complex geology at the KTB site.

Similar estimations have been performed by Huenges et al.(1994). In comparing rock density distribution in the HB derived from borehole gravity data to the distribution of the gneissic and metabasitic cuttings they conclude that the gneissic portion in the upper 6 km outweighs the metabasitic portion. The

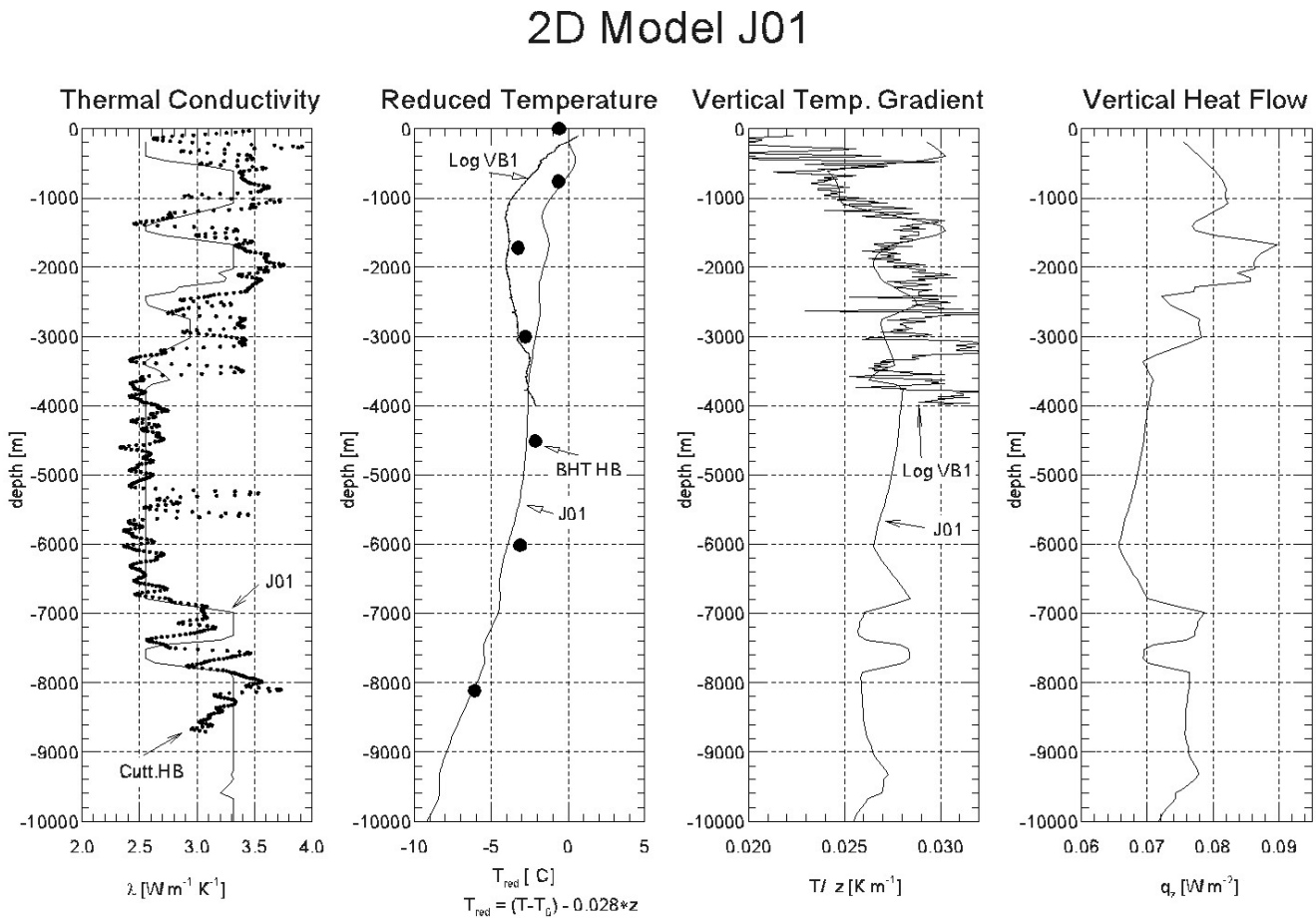

Figure 14. Comparison of the 2-D model J01 with the KTB observables. On the extreme left, the plot shows the measured conductivities from the HB cuttings and a vertical conductivity distribution, which is interpolated from the model to the KTB-HB profile. The next diagram to the right compares the reduced temperature (reduced by a mean gradient of 0.028 K m^{-1}) of the model (run "J01") with BHT measurements in the HB and with the last VB temperature log. The third frame compares the calculated vertical thermal gradient to the vertical gradient profile of the VB temperature log. The last, rightmost frame illustrates the apparent vertical heat flow profile calculated by the model.

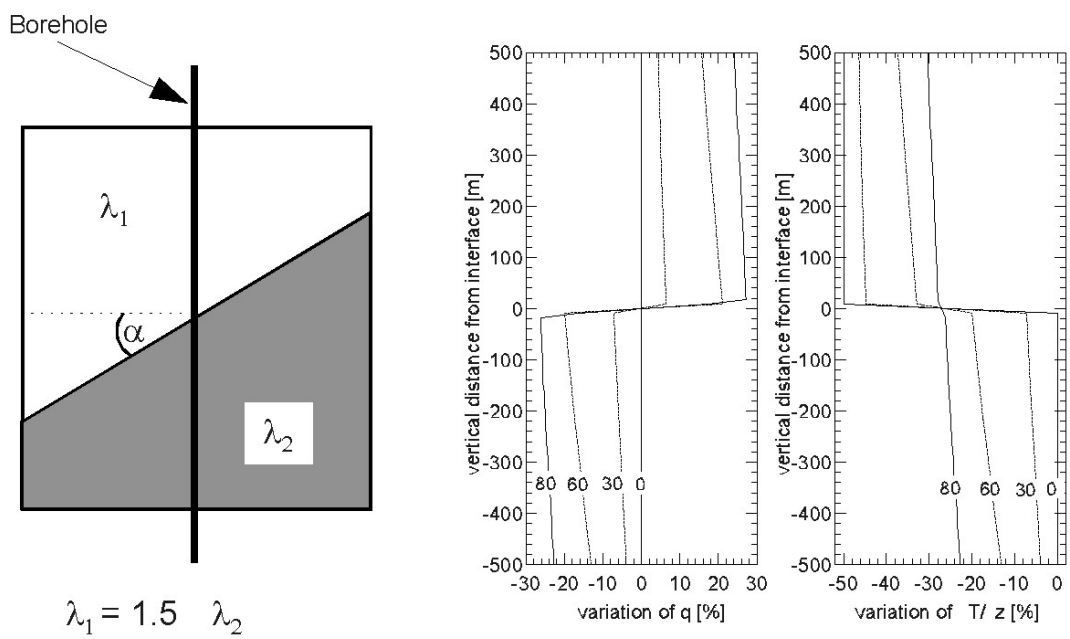

Figure 15. Variation of the vertical components of heat flow q and temperature gradient with dip angle α of the thermal conductivity interface.

differences between the results of the two studies suggest that a further comparative analysis of gravity and geothermal models in distinct depth ranges is necessary for a satisfactory representation of the KTB rock matrix.

8 CONCLUSIONS

The present study has revealed some aspects of data interpretation, which are generally valid for geothermal investigations at sites with steeply dipping geologic structures. It was shown that the uniform temperature gradient of 0.028 K m^{-1} at the KTB site measured in the VB logs and derived from BHT measurements is the result of the strongly dipping alternating gneissic and metabasitic units. The measured gradient in the KTB corresponds to generalised gradient models of the upper crust which predict that the effect of decreasing conductivity with depth (temperature dependence) is counteracted by the cumulative effect of heat production (Chapman & Furlong, 1992). Thermal diffusion seems to be the dominating thermal transport mechanism in the upper crust in the neighbourhood of the KTB site.

The philosophic question whether it is better to limit the number of thermal transport mechanisms or to increase the variability of material distribution is partly answered by our study. Purely diffusive thermal models based on detailed geologic information are well suited to explain the temperature data in the KTB case. The origin of the low temperature gradient (accompanied by low heat flow) in the uppermost 200 m which cannot be simulated with purely diffusive models is partly clarified.

Apart from thermal diffusion, paleoclimatic effects or hydraulic flow due to topography head relief can represent the most important thermal transport mechanisms. The three-dimensional thermo-hydraulic model of the KTB confirms the point of view that topography-driven hydraulic flow is restricted to rather shallow depths which may be due to a permeability decrease and to a fluid density increase with depth. At shallower depths (500 m) high permeabilities ($>10^{-15}$ m^2; about one order of magnitude higher than measured) are required by our analysis. The strong gradient variations in this uppermost zone probably provide the key to the truth, since they are hardly explainable by a paleoclimatic driven diffusive thermal front penetrating slowly into the subsurface. Below 500 m, the rather uniform gradient and the pronounced heat flow variations can now be explained by heat refraction effects.

The geothermal approach has also proven to be a very powerful tool in the analysis of the surrounding material distribution that can be compared to further geophysical investigations like borehole gravimetry. Thus, a further detailed study in co-operation with geologists and geophysicists can reveal the hidden part of the drilled matrix.

ACKNOWLEDGEMENTS

The authors thank the Swiss National Science Foundation for financial support, projects no 21-29803.90 and 2000-039251.93/1. Especially, the authors thank for discussions with C. Clauser, D. Pribnow, U. Harms, E. Huenges and others at the KTB Field Laboratory in Windisch-Eschenbach and at the KTB Project Group in Hannover as well as for the data supply from the KTB Field Laboratory. We also thank F. Medici for the collection and the thermal conductivity measurements of surface rock samples from various quarries in the Oberpfalz. Also the supply of digitised topography data by the Bavarian Geodetic Survey (Bayrisches Landesvermessungsamt) is gratefully acknowledged. Furthermore, the comments of the reviewers are thankfully appreciated. Last but not least, we thank R. Hopkirk for transferring the text into a correct english.

Publication no 859, Institute of Geophysics ETH Zurich.

REFERENCES

Bayrisches Landesvermessungsamt, 1994, Digitales Geländemodell, VM 2255B-3991

Bücker Ch., E. Huenges, E. Lippmann, A. Rauen, K.M. Streit, J. Wienand & H.C. Soffel, 1990, KTB Pilot Hole - Results obtained in the KTB Field-Laboratory, *KTB Report 90-8*, Schweitzerbart'sche Verlagsbuchhandlung, Stuttgart, pp D1-29

Buntebarth, G., 1991, Thermal Properties of KTB Oberpfalz VB Core Samples at Elevated Temperature and Pressure, *Scientific Drilling*, **2**, pp 73-80

Burkhardt H., U. Haak, A. Hahn, H. Hornamand, K. Jäger, A. Stiefel, P. Wägerle, & H. Wilhelm, 1989, Geothermal investigations in the KTB Locations Oberpfalz and Schwarzwald. In Emmermann and Wohlenberg (eds) The German Continental Deep Drilling Programm (KTB), Springer Verlag Berlin pp 433-480

Burkhardt H., K. Erbas, P. Giese, U. Haak, H. Hornamand, E. Huenges, A. Stiefel, H. Wilhelm, G. Zoth, G. Buntebarth & R. Schulz, 1991, The Measured and the Predicted Temperature Profile in the KTB Pilot-hole, *Scientific Drilling*, **2**, pp 244-257

Chapman D.S. & K.P. Furlong, 1992, Thermal State of the Continental Crust, in: D.M. Fountain, R. Arculus & R.W. Kay (edts), Continental Lower Crust, Developments in Geotectonics, **23**, Elsevier

Clauser, C. & E. Huenges, 1993, KTB Thermal Regime and Heat Transport Mechanisms - Current Knowledge, *Scientific Drilling*, **3**, pp 271-281

Clauser, C. & E. Huenges, 1995, Thermal Conductivity of Rocks and Minerals, in: T.J.Ahrens (Edt.), Rock Physics and Phase Relations - a Handbook of Physical Constants, *AGU reference shelf*, Vol.3, pp.105-126, American Geophysical Union, Washington.

Dahlheim H, 1993, Earthquake Parameters and Stress Field Determinations from near the KTB-Drill Site, *KTB Report 93-2*, Schweitzerbart'sche Verlagsbuchhandlung, Stuttgart, pp 211-212

Emmermann R., 1989, The KTB Pilot Hole: Tectonic Setting, Technical Data and First Results, in Emmermann and Wohlenberg (eds) The German Continental Deep Drilling Programm (KTB), Springer Verlag Berlin pp 527-553

Freeze R.A. & J.A. Cherry, 1979, Groundwater, Prentice Hall, New Jersey, USA, pp 172-173

Hirschmann G., 1992, Das Bruchstörungsmuster im KTB-Umfeld, *KTB Report 92-3*, Schweitzerbart'sche Verlagsbuchhandlung Stuttgart, pp 85-124

Hirschmann G., 1993, Zur Geologie der KTB Oberpfalz, *Z. geol. Wiss.*, **21(1/2)**, pp 105-116

Huenges E. & G. Zoth, 1991, KTB Oberpfalz VB: Temperature, Thermal Conductivity and Heat flow density, *Scientific Drilling*, **2**, pp 81-89

Huenges E., 1993, Profiles of Permeability and Formation-Pressure down to 7.2 km, *KTB-Report 93-2*, Schweitzerbart'sche Verlagsbuchhandlung Stuttgart, pp 279-285

Huenges E., U. Harms, C. Clauser & D. Pribnow, 1994, Observed Temperature and Heat Flow Density in the KTB: Possible Sources, Proc. VIIth Int. Sympos. on the Observation of the Continental Crust Through Drilling, April 25-30, Santa Fe USA, pp 118-121, DOSECC Continental Scientific Drilling Program, Texas A&M Univ., College Station, USA

Jobmann M., 1990, Thermischer Injektionstest und Temperaturmessung nach sechsmonatiger Standzeit in der KTB Oberpfalz, *KTB Report 90-6a*, Schweitzerbart'sche Verlagsbuchhandlung Stuttgart, pp 229-243

Jobmann K. & C. Clauser, 1994, Heat Advection Versus Conduction at the KTB: Possible Reasons for Vertical Variations in the Heat Flow Density, *Geophysical Journal International*, **119**, pp 44-68

Kessels W., J. Kück & G. Zoth, 1992, Hydraulische Untersuchungen in der Bohrung KTB-Oberpfalz HB bis 5000 m, *KTB Report 92-1*, Schweitzerbart'sche Verlagsbuchhandlung Stuttgart, pp 169-205

Kohl T., R.J. Hopkirk, K.F. Evans & L. Rybach, 1993, FRACTure - A New Tool to Simulate Coupled Processes in Geosciences, In: K. Morgan, E. Oñate, J. Periaux, J. Peraire, O.C. Zienkiewicz (Eds), Finite Elements in Fluids, Pineridge Press, pp 949-958

Kohl T & L. Rybach, 1994, Modeling the Heat Flow Field in the Surrounding of the KTB drill site, Proc. VIIth Int. Sympos. on the Observation of the Continental Crust Through Drilling, April 25-30, Santa Fe USA, pp 114-117, DOSECC Continental Scientific Drilling Program, Texas A&M Univ., College Station, USA

Kopecký L., 1986, Geological Development and Block Structure of the Cenozoic Ohre Rift (Czechoslovakia), Proc. of the 6th Intern. Conf. on Basement Tectonics, pp 114-124

Medici F., 1994, Wärmeleitfähigkeitsmessungen an Oberflächengesteinen der KTB, Internal Report, Institut für Geohysik, ETH Zürich, Switzerland

Phillips S.L., A. Igbene, J.A. Fair, H. Ozbek & M.Tavan, 1981, A Technical Databook for Geothermal Energy Utilization, Lawrence Berkeley Laboratory, Report No. LBL-12810, USA

Pribnow D., 1994, Ein Vergleich von Bestimmungsmethoden der Wärmeleitfähigkeit unter Berücksichtigung von Gesteinsgefügen und Anisotropie, Fortschritt-Berichte VDI Reihe 19, No. 75, VDI Verlag Düsseldorf, Germany

Rybach L., 1988, Determination of Heat Production Rate, in R. Haenel, L. Rybach & L. Stegena, Handbook of Terrestrial Heat-Flow Density Determination, Kluwer Acad. Publ., Dordrecht, pp 125-142

Rybach L., 1992, An Attempt to Interpret the Temperature Profile of the KTB Pilot Drill Hole (Germany) by Paleoclimatic Considerations, *Paleogr., Paleoclimatol., Palaeoecol., (Global Planet. Change Sect.)*, **98**, pp 193-197

Šibrava V. & P. Havlicek, 1980, Radiometric Age of Plio-Pleistocene Volcanic Rocks of the Bohemian Massif, *Bulletin of the Geological Survey, Prague*, **55**(3), pp 129-140

Stiefel A., 1990, Gegenstrom Wärmetauscher-Experiment und Temperaturangleich in der KTB Oberpfalz VB vom 09. bis 19. März 1990, *KTB Report 90-6a*, Schweitzerbart'sche Verlagsbuchhandlung Stuttgart, pp 259-281

Weinlich F.H., K. Bräuer, H. Kämpf, 1993, G. Strauch & S. Weise, Gasgeochemical Investigations on Mineral Springs along a Cross-Section through the Eger Rift, *KTB-Report 93-2*, Schweitzerbart'sche Verlagsbuchhandlung Stuttgart, pp 417-421

Adapted from *Geophys. J. Int.*, **124**, *756-776*